Infrared Studies on Films of Carbosilazane and Siloxazane Networks

B. C. Trasferetti,[†,§] R. V. Gelamo,[†] F. P. Rouxinol,[†] M. A. Bica de Moraes,*[,†] and C. U. Davanzo[‡]

Instituto de Física Gleb Wataghin, Universidade Estadual de Campinas, Caixa Postal 6165, 13.083-970, Campinas SP, Brazil, and Instituto de Química, Universidade Estadual de Campinas, Caixa Postal 6154, 13.084-971, Campinas SP, Brazil

Received February 12, 2005. Revised Manuscript Received April 20, 2005

The present work describes the effects of diluting hexamethyldisilazane (HMDSN) vapor either in pure argon or in oxygen−argon mixtures on the solid film deposited from the resulting plasma. Such a dilution provides a manner of incorporating controllable amounts of Si−O groups into the solid film. The characterization of the films investigated here was made by longitudinal and transverse optical (LO and TO, respectively) functions in the mid-infrared calculated through the Kramers-Krönig analysis of transmittance spectra. The infrared analysis showed that the films were formed by silicon-centered distorted tetrahedra of the following type: $Si(CH_3)_xBU_{(2-0.5x)}$, where $0 \leq x \leq 3$ and BU stands for bridging unit. For the sample deposited in the absence of O_2 in the discharge, BU = CH_2 and NH; for the samples deposited with an O_2 flow rate (f_{O2}) of 2.5 and 10 sccm, BU = CH_2, NH, and O; and for the sample deposited with f_{O2} of 20 sccm, BU = NH and O. The Δ_{LO-TO} for the Si−O asymmetrical stretching increased from 0 ($f_{O2} = 0$ sccm) to 73 cm^{-1} ($f_{O2} = 20$ sccm), while for the Si−N asymmetrical stretching it decreased from 20 ($f_{O2} = 0$ sccm) to 3 cm^{-1} ($f_{O2} = 20$ sccm). These observations signal an increase in the Si−O−Si network and a decrease in the Si−NH−Si network as the oxygen flow increased. An interesting conclusion drawn from our analysis of the Si−H stretching mode position and Δ_{LO-TO} for the AS1 band is that the films deposited in the presence of O_2 are not structurally homogeneous, but have domains with different proportions of O bridges.

I. Introduction

Plasma-enhanced chemical vapor deposition (PECVD) is a very versatile technique that permits the production of a wide range of materials according to the deposition conditions.[1] Besides carbonaceous materials, such as highly cross-linked organic polymers[2,3] and diamond-like coatings,[4,5] PECVD has been amply used in the production of silicon-based materials from organosilicon molecular precursors.[6−15] One of its advantages is the possibility of synthesizing Si-based materials with controlled amounts of a determined element or chemical group. This can be accomplished in several ways: (i) diluting the precursor molecules in different gases;[9,11,12] (ii) heating the substrate;[11] (iii) collecting the film in different regions of the plasma or even out of the plasma;[8] etc. Other advantages are the following: (i) PECVD yields films with excellent adherence properties;[9−11] (ii) it offers a lower deposition temperature and higher deposition rate by plasma assistance than the higher deposition temperature and lower deposition rate required in conventional CVD;[11] (iii) it offers the prospect of coating substrates with complex topologies and small dimensions, such as neurological electrodes;[10] etc.

The present work describes the effects of diluting hexamethyldisilazane (HMDSN) vapor either in pure argon or in oxygen−argon mixtures on the solid film deposited from the resulting plasma. Such a dilution provides a manner of incorporating controllable amounts of Si−O groups into the solid film. This type of film finds applications in surface modifications of materials which are not stable at high

* Corresponding author. E-mail: bmoraes@ifi.unicamp.br.
† Instituto de Física Gleb Wataghin, Universidade Estadual de Campinas, Caixa Postal 6165, 13.083-970, Campinas SP, Brazil.
‡ Instituto de Química, Universidade Estadual de Campinas, Caixa Postal 6154, 13.084-971, Campinas SP, Brazil.
§ Present address: Departamento de Polícia Federal, Superintendência Regional no Piauí, Setor Técnico-Científico, Avenida Maranhão, 1022/N, 64.000-010, Teresina PI, Brazil.

(1) d'Agostino, R., Ed.; *Plasma Deposition, Treatment and Etching of Polymers*; Academic Press: San Diego, CA, 1990; p 163.
(2) Chou, L. H. *J. Appl. Phys.* **1992**, *72*, 2027.
(3) Durrant, S. F.; Castro S. G.; Cisneros, J. I.; Da Cruz, N. C.; Bica de Moraes, M. A. *J. Vac. Sci. Technol.* **1996**, *14*, 118.
(4) Ebihara, K.; Ikegami, T.; Matsumoto, T.; Nishimoto, H.; Harada, K. *J. Appl. Phys.* **1989**, *66*, 4996.
(5) Lee, J. H.; Kim, D. S.; Lee, Y. H.; Farouk, B. *J. Mater. Sci* **1995**, *14*, 1132.
(6) Pai, P. G.; Chao, S. S.; Takagi, Y.; Lukovsky, G. *J. Vac. Sci. Technol. A* **1986**, *4*, 689.
(7) Fracassi, F.; d'Agostino, R.; Favia, P.; van Sambeck, M. *Plasma Sources Sci. Technol.* **1993**, *2*, 106.
(8) Wróbel, A. M.; Wickramanayaka, S.; Nakanishi, Y.; Fukuda, Y.; Hatanaka, Y. *Chem. Mater.* **1995**, *7*, 1403.
(9) Da Cruz, N. C.; Durrant, S. F.; Bica de Moraes, M. A. *J. Polym. Sci., Part B: Polym Phys.* **1998**, *36*, 1873.
(10) Pryce Lewis, H. G.; Edell, D. J.; Gleason, K. K. *Chem. Mater.* **2000**, *12*, 3488.
(11) Kuo, D. H.; Yang, D. G. *J. Electrochem. Soc.* **2000**, *147*, 2679.
(12) Magni, D.; Descheneaux, C.; Hollenstein, C.; Creatore, A.; Fayet, P. *J. Phys. D: Appl. Phys.* **2001**, *34*, 87.
(13) Trasferetti, B. C.; Davanzo, C. U.; Bica de Moraes, M. A. *J. Phys. Chem B* **2003**, *107*, 10699.
(14) Trasferetti, B. C.; Davanzo, C. U.; Bica de Moraes, M. A. *Macromolecules* **2004**, *37*, 459.
(15) Trasferetti, B. C.; Gelamo, R. V.; Rouxinol, F. P.; Bica de Moraes, M. A.; Gonçalves, M. C.; Davanzo, C. U. *Chem. Mater.* **2004**, *16*, 567.

10.1021/cm050319o CCC: $30.25
Published on Web 08/02/2005

temperatures, such as increasing the hardness of plastics and improvement of conventional polymers.[7] We also speculate that plasma-polymerized organocarbosilazane films can be used as silicon carbonitride preceramic materials (see refs 16−18 on the polymer−ceramic convertion of polysilazanes). HMDSN has also been used as the silicon source in the production of thick SiO_2 films.[11] In that case, nitrogen incorporation in the film was suppressed by diluting the precursor vapor in CO_2 and H_2 and heating the substrate at 300−450 °C.

The characterization of the films investigated here was made by longitudinal and transverse optical (LO and TO, respectively) functions[19−23] in the mid-infrared calculated through the Kramers-Krönig analysis of transmittance spectra.[24,25] As reported in our previous papers,[13,14] the analysis of these functions can give more insight into the structure of these materials than the conventional analysis of transmission maxima. This is because the splitting between LO and TO maxima for a given vibrational mode is sensitive to the density of the corresponding oscillators within the solid structure.[26] However, it is mandatory that the oscillator strength is relatively high. Therefore, a significant LO-TO splitting is expected for polar-bond-related modes, such as Si−O,[13,14,27−33] Ti−O,[34−37] and W−O[38] asymmetrical stretchings, but is not for common organic-group-related modes, such as C−H stretchings or deformations.

II. Experimental Section

Film deposition was carried out in a stainless steel vacuum chamber fitted with two horizontal parallel plate water-cooled electrodes of 11 cm diameter. The upper electrode was connected to a radio frequency generator (40 MHz, 100 W max. power) while the lower was grounded. The chamber was pumped by a 150 m^3/h Roots pump backed by a 22 m^3/h rotary vane pump. A Pirani manometer was used for pressure readings. Argon was admitted to the chamber using a precision electronic mass flow meter. The source of HMDSN (Aldrich) vapor, a 60 cm^3 glass bulb containing liquid HMDSN, was connected to the chamber via a precision leak valve. To avoid a fall in temperature of the liquid during evaporation, the cell was immersed in a room-temperature water bath. As substrates, we used KBr disks for the IR analysis, silicon wafers for the refractive index measurements in the visible range, and glass slides for thickness measurements. The thicknesses of the films were determined with a Dektak profilemeter. Table 1 summarizes the deposition parameters, thicknesses and refractive indices, of the five samples that are discussed in this paper. The samples were labeled according to the gases (and their flow rates) in which HMDSN was diluted. For all depositions, the partial pressure of HMDSN was kept at 2.5 Pa.

Table 1. Deposition Parameters, Thicknesses, and Refractive Indices of the Investigated Films

sample[a]	f_{O2} (sccm)	F_{Ar} (sccm)	d (nm)	n (λ = 633 nm)
HAr	0	40	565	1.55
HO2.5	2.5	37.5	581	1.53
HO10	10	30	534	1.46
HO20	20	20	401	1.43

[a] These labels correspond to the deposition conditions. Each batch was constituted of four films deposited on (i) a KBr disk, (ii) on a glass slide, (iii) on an aluminum-coated glass slide, and (iv) on a silicon wafer.

Refractive indices were obtained from measurements performed through single wavelength ellipsometry (SWE) in a Rudolph Model Auto EL Ellipsometer equipped with a laser of wavelength 632.8 nm.

Elemental analyses of the films were made using Rutherford backscattering spectroscopy (RBS) at the Laboratory for Analysis of Materials by Ion Beams−LAMFI of the Institute of Physics, University of São Paulo. RBS was used to detect Si, C, N, and O using a beam of singly ionized 2.4 MeV helium atoms aligned normal to the film surface with detection at 10° off-normal. Single crystals (100) Si wafers were used as substrates. From RBS data, the areal densities of Si-, C-, N-, and O-atoms of the film were obtained using the SIMNRA computational program.[39]

Both the infrared transmission and reflection−absorption spectra were measured for all samples in a Bomen MB-101 FT-IR spectrometer equipped with a DTGS detector. The spectral range covered was 400−5000 cm^{-1}. Each spectrum was the result of co-adding 64 scans collected at 4 cm^{-1} resolution, in the transmission mode. All transmission measurements were referenced to a bare KBr disk and carried out at room temperature.

The data analysis we use here has been described elsewhere.[13] In brief, the optical constant (refractive and absorption indices, n and k, respectively) determinations were carried out through the Kramers-Krönig analysis (KKA) of transmission data (see ref 22). k is determined directly from the absorption spectrum of a thin film of known thickness deposited on a transparent material. From the spectrum of k and the value of n_∞ (the refractive index of the material in the visible range), n can be determined by means of KKA. We used an algorithm that is described in ref 24.

For nonmagnetic materials, $\tilde{\epsilon} = (n + ik)^2$, where $\tilde{\epsilon}$ is the complex dielectric function. TO and LO functions, whose maxima correspond to the vibrational modes TO and LO, respectively, can be obtained from[22]

$$\text{TO-function} = \text{Im}(\tilde{\epsilon})$$

$$\text{LO-function} = \text{Im}(-1/\tilde{\epsilon})$$

(16) Han, H. N.; Lindquist, D. A.; Haggerty, J. S.; Seyferth, D. *Chem. Mater.* **1992**, *4*, 705.
(17) Breuning, T. *J. Anal. Appl. Pyrol.* **1999**, *49*, 43.
(18) Schiavon, M. A.; Sorarù, G. D.; Yoshida, I. V. P. *J. Non-Cryst. Solids* **2002**, *304*, 76.
(19) Berreman, D. W. *Phys. Rev.* **1963**, *130*, 2193.
(20) Kittel, C. *Introduction to Solid State Physics*, 7th ed.; John Wiley & Sons: New York, 1996.
(21) Blakemore, J. S. *Solid State Physics, Second Edition*; Cambridge University Press: Cambridge, 1995.
(22) Ten, Y.-S.; Wong, J. S. *J. Phys. Chem.* **1989**, *93*, 7208.
(23) Harbecke, B.; Heinz, B.; Grosse, P. *Appl. Phys. A* **1985**, *38*, 263.
(24) Hawranek, J. P.; Jones, R. N. *Spectrochim. Acta* **1976**, *32*, 99.
(25) Yamamoto, K.; Ishida, H. *Vib. Spectrosc.* **1994**, *8*, 1.
(26) Jones, L. H.; Swanson, B. I. *J. Phys. Chem.* **1991**, *95*, 2701.
(27) Kirk, C. T. *Phys. Rev. B* **1988**, *38*, 1255.
(28) Almeida, R. M. *Phys. Rev. B* **1992**, *45*, 161.
(29) Guiton, T. A.; Pantano, C. G. *Colloid Surf. A* **1993**, *74*, 33.
(30) Kamitsos, E. I.; Patsis, A. P.; Kordas, G. *Phys. Rev. B* **1993**, *48*, 12499.
(31) Sarnthein, J.; Pasquarello, A.; Car, R. *Science* **1997**, *275*, 1925.
(32) Pasquarello, A.; Car, R. *Phys. Rev. Lett.* **1997**, *79*, 1766.
(33) Trasferetti, B. C.; Davanzo, C. U. *Appl. Spectrosc.* **2000**, *54*, 502.
(34) Trasferetti, B. C.; Davanzo, C. U.; Da Cruz, N. C.; Bica de Moraes, M. A. *Appl. Spectrosc.* **2000**, *54*, 687.
(35) Trasferetti, B. C.; Davanzo, C. U.; Zoppi, R. A.; Da Cruz, N. C.; Bica de Moraes, M. A. *Phys. Rev. B* **2001**, *64*, 125404.
(36) Trasferetti, B. C.; Davanzo, C. U.; Zoppi, R. A. *Electrochem. Commun.* **2002**, *4*, 301.
(37) Zoppi, R. A.; Trasferetti, B. C.; Davanzo, C. U. *J. Electroanal. Chem.* **2003**, *544*, 47.
(38) Trasferetti, B. C.; Rouxinol, F. P.; Gelamo, R. V.; Bica de Moraes, M. A.; Davanzo, C. U.; de Faria, D. L. A. *J. Phys. Chem. B* **2004**, *108*, 12333.
(39) Mayer, M. *SIMNRA User's Guide*; report IPP 9/113; Max-Planck-Institut für Plamaphysik: Garching, Germany, 1997.

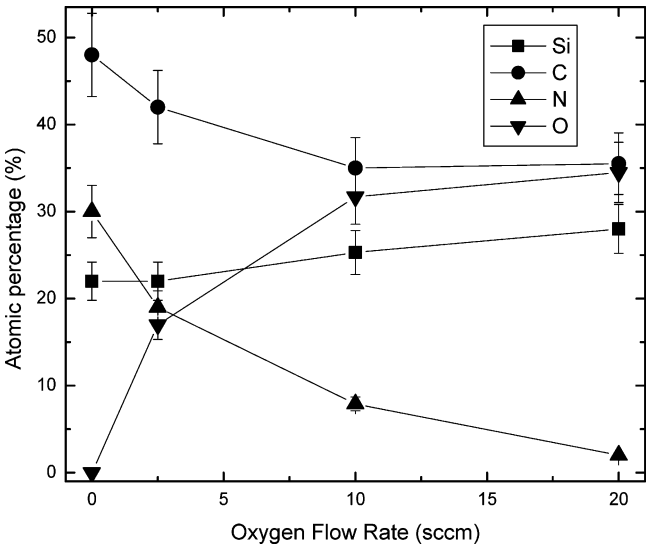

Figure 1. Atomic percentages as calculated from simulations of Rutherford backscattering spectra.

III. Results and Discussion

III.A. Elemental Composition. Figure 1 shows the atomic percentages as calculated from simulations of the Rutherford backscattering spectra. It is important to remark that the hydrogen content cannot be directly accessed by RBS. The analysis of Figure 1 evidences important trends of elemental incorporation into the solid film as the O_2 to HMDSN flow rate ratio increased in the plasma in the flow rate ratio range investigated: (i) carbon incorporation decreases at a decreasing rate down to around 35%; (ii) nitrogen incorporation decreases at a decreasing rate down to almost zero; (iii) oxygen incorporation increases at a decreasing rate up to around 35%; and (iv) silicon incorporation increases almost linearly.

III.B. Infrared Spectral Data and Chemical Groups Forming the Solid Films. As described in the Experimental Section, the normal incidence transmittance spectra of the films deposited on KBr were Kramers-Krönig-transformed into the corresponding optical constants spectra. From these spectra, we have calculated the LO and TO functions for all samples. Since the bands occurring in the low-frequency region of the spectra of our films are much more intense than those occurring in the high-frequency region, we are presenting the spectra in two different Figures. Figure 2 shows both the LO and TO functions for all samples in the low-frequency region and Figure 3 shows only the TO function for all samples in the high-frequency region. In the latter, only the TO functions were presented because no LO-TO splitting was observed for the bands within the spectral region shown.

Table 2 summarizes both the LO and the TO bands for all samples and their assignments. Such assignments were made from the literature and were based on the values of the TO frequencies since all the literature data on IR spectroscopy is based, on one hand, on normal-incidence transmittance experimental studies and, on the other hand, on theoretical studies on model gaseous molecules. In the present case, we have based our band assignments on the theoretical studies carried out by McKean and co-workers

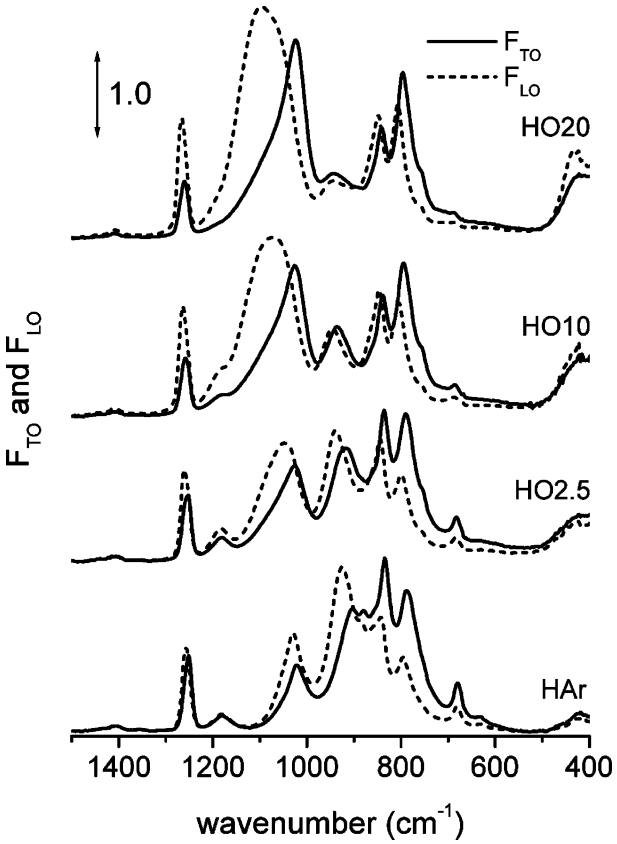

Figure 2. LO and TO functions (low-frequency region) for all samples calculated according to the procedure outlined in section II. Note that the intensity of the LO functions was multiplied by a factor of 5 to match the TO function intensities.

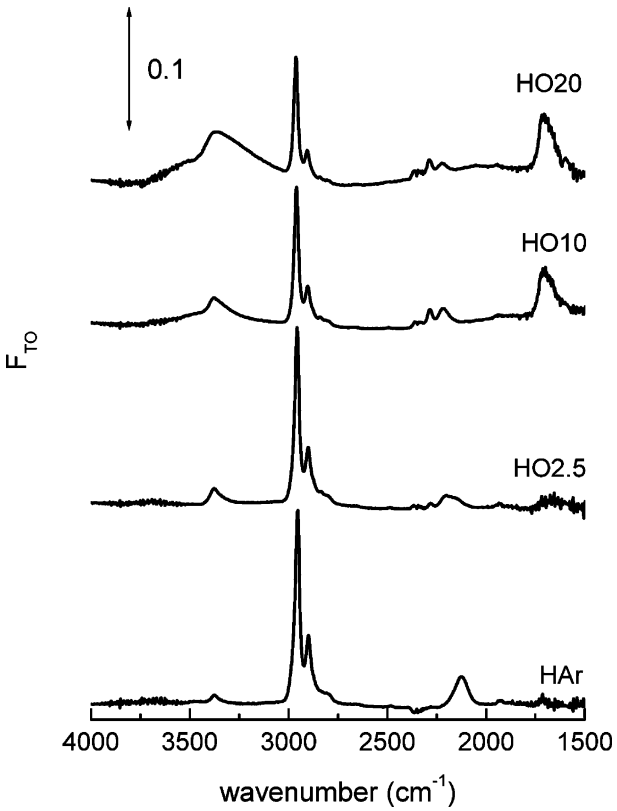

Figure 3. TO functions (high-frequency region) for all samples, calculated by the same procedure as in Figure 1.

for model molecules such as hexamethyldisiloxane (HMDSO) $[(Me)_3Si-O-Si(Me)_3]$,[40] HMDSN $[(Me)_3Si-$

Table 2. Infrared Band Assignments from the Literature

band position (cm^{-1})									
HAr		HO2. 5		HO10		HO20			
TO	LO	TO	LO	TO	LO	TO	LO	assignment[a]	references
							~420	ρ_{Si-O} in Si−O−Si	13, 14
633	633							?	
680	682	683	684	686	686	686	686	$\nu_{S,Si-C3}$	41
787	797	790	800	794	804	797	806	ρ_{Me},ν_{SiC} in Si−Me_2	45, 46
833	844	836	845	838	848	841	849	ρ_{Me},ν_{SiC} in Si−Me_3	45, 46
880	880								50, 51
905	925	917	939	935	946	942	945	$\nu_{AS,SiN}$ in Si−N−Si	41, 50, 51
1022	1029							ω_{CH2} in Si−CH_2−Si	47−49, 54
		1026	1046	1027	1075	1025	1098	$\nu_{AS,SiO}$ in Si−O−Si	45, 46
1182	1182	1180	1182	1180 (sh.)	1180 (sh.)			δ_{N-H}	41, 50, 51
1252	1257	1254	1260	1259	1264	1260	1266	$\delta_{S,Me}$ in Si−Me_x	45, 46
1357	1357	1355	1355	1356	1356			γ_{CH2} in Si−CH_2−Si	47−49, 54
1405	1405	1406	1406	1406	1406	1408	1408	$\delta_{AS,Me}$ in Si−Me_x	45, 46
				1708	1708	1708	1708	$\nu_{C=O}$	52
2128	2128	2200	2200	2216	2216	2223	2223	ν_{Si-H}	53, 55
		2281	2281	2284	2284	2287	2287	ν_{Si-H}	53, 55
2900	2900	2902	2902	2902	2902	2905	2905	$\nu_{S,C-H}$ in Si−Me_x	45, 46
2953	2953	2956	2956	2959	2959	2962	2962	$\nu_{AS,C-H}$ in Si−Me_x	45, 46
3375	3375	3377	3377	3379	3379	3365	3365	ν_{N-H}	45, 46

[a] ν, δ, ρ, ω, and γ denote stretching, bending, rocking, wagging, and scissoring modes, respectively; AS and S denote asymmetric and symmetric vibrations.

Table 3. Si−N Asymmetrical Stretching Position for Different Si−N Bond Configurations, from the Literature

type of material	formula	$\nu_{AS,Si-N}$ position (cm^{-1})	references
hexamethyldisilazane	$(CH_3)_6Si_2NH$	932	41
silicon nitride	Si_3N_4	840	50, 51
silicon diimide	$Si(NH)_2$	880	50, 51
silicon oxynitride	SiO_xN_y	840 for NSi_3 groups	56
		960 for NSi_2 groups	56

NH−$Si(Me)_3$],[41] trimethylsilane [$HSi(Me)_3$],[42] and disilylmethane [$H_3Si-CH_2-SiH_3$][43] or on the experimental studies carried out by Marchand and co-workers,[44] by Anderson and Lee Smith,[45,46] and by Sugahara and co-workers.[47−49] A detailed discussion on all the observed chemical groups forming the solids deposited is presented below.

1. Si−N Groups. Before we start discussing the presence of Si−N bonds in the films we are investigating, let us make a very brief review on the infrared studies on materials and molecules bearing Si−N bonds. Since the most intense and reliable band for this group is the asymmetrical stretching for the Si−N group ($\nu_{AS,Si-N}$), Table 3 summarizes the main examples of materials containing Si−N bonds, their simplified formulas, observations on $\nu_{AS,Si-N}$, and the references that will serve as a basis for our discussion.

As can be seen from Table 3, the $\nu_{AS,Si-N}$ is strongly dependent on the bonding configurations of nitrogen. In the spectrum of the HAr sample, we observed a band at 880 and another at 905 cm^{-1}. Therefore, it seems that there are Si−N bonds in two different local configurations in this sample. We suppose that these configurations are related to the number of NH bridges bonded to the silicon atom in silicon-centered distorted tetrahedra. The band at 880 cm^{-1} corresponds to the tetrahedrum of a silicon bonded to four NH bridges such as those present in $Si(NH)_2$[50,51] and that at 905 cm^{-1} denotes silicon bonded to 2 or 3 NH bridges.

The presence of oxygen in the discharge brings interesting changes in the position of the $\nu_{AS,Si-N}$ band. The band at 880 cm^{-1} disappears and the band at 905 cm^{-1} blue-shifts up to 942 cm^{-1} as the oxygen feed increases from 0 to 20 sccm, which denotes a decrease in the number of NH bridges connected to the same silicon atom since the position of the band migrates to a region closer to that observed for the HMDSN molecule.[41] It is also important to stress that, besides the blue-shift, a decrease in the intensity of the band is observed with the increase in the oxygen flow rate, which denotes a depletion in the amount of Si−N groups.

2. Si−O. From Figure 1, the most prominent TO bands for samples deposited in the presence of oxygen, at around 1026 cm^{-1}, are assigned to the Si−O−Si asymmetrical stretching mode.[46] It will be termed AS1 mode, in analogy to v-SiO_2, for which it lies at 1072 cm^{-1}.[27,33] The appearance of the AS1 modes at frequencies lower than that of v-SiO_2 has also been observed for structures bearing a suboxide bonding arrangement, e.g., the SiO_x films deposited by PECVD investigated by Lucovsky and co-workers[53] and Pai and co-workers.[6] Furthermore, Si−O−Si absorption bands within the range 1055−1024 cm^{-1} have been observed for

(40) McKean, D. C. Unpublished results.
(41) Fleischer, H.; McKean, D. C. *J. Phys. Chem. A* **1999**, *103*, 727.
(42) McKean, D. C. *Spectrochim. Acta A* **1999**, 55, 1485.
(43) McKean, D. C.; Davidson, G.; Woodward, L. A. *Spectrochim. Acta A* **1970**, *26*, 1815.
(44) Marchand, A.; Valade, J.; Forel, M.-T.; Josien, M.-L.; Calas, R. *J. Phys. Chim.* **1962**, *59*, 1142.
(45) Lee Smith, A.; Anderson, D. R. *Appl. Spectrosc.* **1984**, *38*, 822.
(46) Anderson, D. R. In *Analysis of silicones*; Smith, A. L., Ed.; John Wiley & Sons: New York, 1974.
(47) Sugahara, S.; Usami, K.; Matsumura, M. *Jpn. J. Appl. Phys.* **1999**, *38*, 1428.
(48) Sugahara, S.; Kadoya, T.; Usami, K.; Hattori, T.; Matsumura, M. *J. Electrochem. Soc.* **2001**, *148*, F120.
(49) Usami, K.; Sugahara, S.; Kadoya, T.; Matsumura, M. Proc. 7th. International Symposium on Quantum Effect Electronics, Tokyo Institute of Technology, 2000 (http://www.pe.titech.ac.jp/qee_root/symposium/ symposium2000program.htm).
(50) Tsu, D. V.; Lucovsky, G.; Mantini, M. J. *Phys. Rev. B* **1986**, *33*, 7069.
(51) Tsu, D. V.; Lucovsky, G. *J. Vac. Sci. Technol. A* **1986**, *4*, 480.
(52) Bellamy, L. J. *The Infra-Red Spectra of Complex Molecules*; Chapman & Hall: London, 1975.
(53) Tsu, D. V.; Lucovsky, G.; Davidson, B. N. *Phys. Rev. B* **1989**, *40*, 1795.

polymeric siloxanes. The fact that the bands do not exhibit a clear splitting of the AS1 mode indicates a network rather than a polymeric character.[10]

Another distinguishing Si−O feature is the Si−O bond rocking mode. For thermal SiO_2, it is located at 450 cm^{-1}.[27,33] A red-shift is also expected for SiO_x-like materials.[53] We could not determine precisely the position of the maxima of the TO function of the samples HO2.5, HO10, and HO20, either because of the low sensitivity of the spectrometric detector in this wavenumber region or the possibility that the maxima lie below 400 cm^{-1}.

3. $Si(CH_3)_x$. Several bands related to methyl groups bonded to silicon atoms are present in our spectra. The most obvious one is the asymmetrical deformation of methyl groups in $Si(CH_3)_x$ groups.[46] For sample HAr, it was at 1252 cm^{-1}, blue-shifting as the oxygen flow rate increased, up to 1260 cm^{-1}, for sample HO20. Analogous to Si−H stretching, this band is sensitive to the presence of electronegative atoms such as oxygen bonded to the same silicon atom to which the methyl group is bonded.[13,14]

We also observed in all spectra a very low intensity band at 1400 cm^{-1}, which is attributed to the symmetrical deformation of methyl groups in $Si(CH_3)_x$ groups.[46] Both the frequencies of the symmetrical and asymmetrical C−H stretchings in methyl groups (∼2900 and ∼2953 cm^{-1}, respectively, for sample HAr) are also very characteristic of methyl groups bonded to silicon.[46] We also observed small blue-shifts for both bands as the oxygen flow rate increased.

In the 650−900 cm^{-1} range, we observed several bands that are related to Si−C stretchings and methyl rockings in $Si(CH_3)_x$ groups (see Table 2).[41] These bands are useful for characterizing the presence of monomethyl-, dimethyl-, and trimethyl-substituted silicon.[46] An important piece of information that can be drawn from these data is that a significant amount of $Si(CH_3)_3$ groups are incorporated in the films deposited in the absence of oxygen. This is easily inferred if we consider the band at ∼680 cm^{-1}, which is related to $Si(CH_3)_3$ groups and is known to be very weakily IR-active.[41] Therefore, its very observation is proof that a significant amount of $Si(CH_3)_3$ groups are present in the solid film. Since this group is a constitutive moiety of the precursor molecule, this is indirect evidence that the degree of fragmentation is higher in the presence of oxygen. It is interesting to note that the intensity of the band related to $Si(CH_3)_3$ groups decreases exponentially while that related to $Si(CH_3)_2$ groups increases linearly as shown in Figure 4. This observation also corroborates the above-mentioned inference related to an increase in the fragmentation of the monomer propiciated by the increase in the amount of reactive oxygen species in the discharge.

4. Si−CH_2−Si. Owing to the absence of O_2 in the discharge, sample HAr presents characteristics that are different from those of the other films. The TO band observed at 1022 cm^{-1} can be assigned to the wagging mode (ω) of methylene in Si−CH_2−Si groups,[43] which is the basis of the skeleton of the materials known as polycarbosilanes. In addition to this band, another important fingerprint of Si−CH_2−Si groups is observed at ∼1350 cm^{-1}.[43,54] Figure 5 shows an amplification of the TO function of the films in this region. It is a band assigned to the scissoring deformation (γ) of methylene groups, whose intensity decreases and extinguishes as the oxygen flow rate increases. From these observations, it can be supposed that Si−CH_2−Si groups are important constituents of the skeleton of HAr. The issue of Si−$(CH_2)_n$−Si-group-containing silica structures (with $1 \leq n \leq 3$) has recently been investigated by Sugahara and coworkers.[47−49] For the film with $n = 1$, they did observe a band at ∼1360 cm^{-1}, which was attributed to γ_{CH2} in Si−(CH_2)−Si. It is important to stress that this band was not

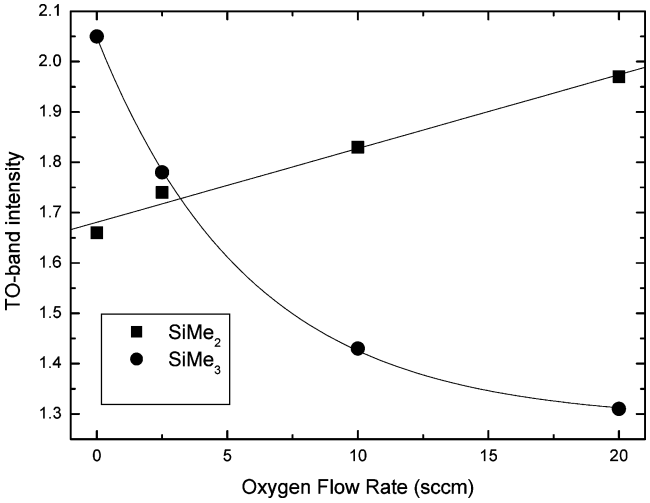

Figure 4. Intensity of the $SiMe_3$- and $SiMe_2$-related bands as a function of the oxygen flow rate. The straight lines are guides for the eye.

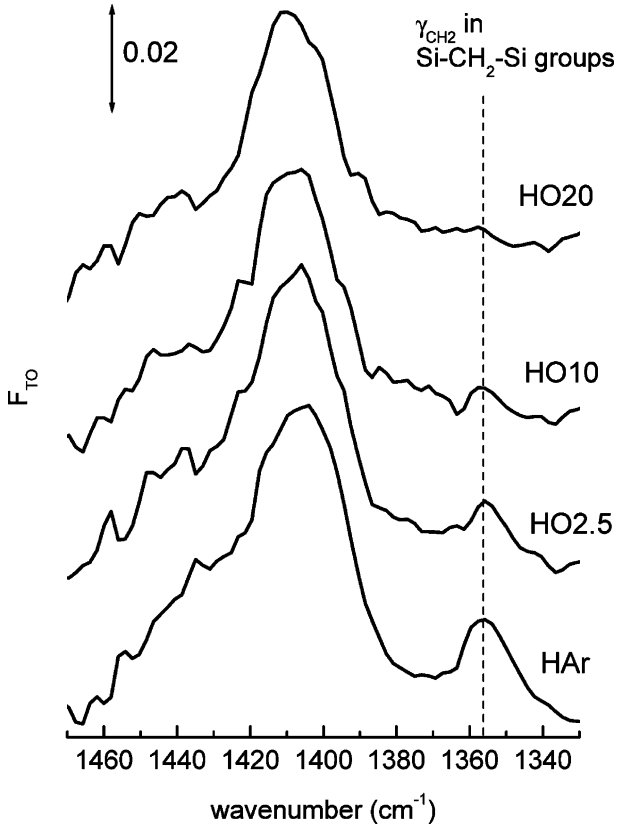

Figure 5. Magnification of the TO functions for all samples in the region of CH_2 wagging in Si−CH_2−Si groups.

(54) Scarlete, M.; Brienne, S.; Butler, I. S.; Harrod, J. F. *Chem. Mater.* **1994**, *6*, 977.

accompanied by the methylene C−H stretching bands. However, for films with $n = 2$, they have not observed the band at ∼1360 cm^{-1} and started to observe both C−H stretchings and two bands at 1280 and 1160 cm^{-1}, which are related to $Si-CH_2CH_2-Si$.[46] Therefore, it seems that the presence of successive methylene groups plays an important role in the intensity and the position of CH_2-related bands.

From the spectrum of Figure 5, it can be affirmed that the formation of disilylethylene groups ($SiCH_2CH_2Si$) in film HAr did not occur since the spectrum did not show the characteristic in-phase wagging vibration of the two methylene groups, which lies between 1180 and 1120 cm^{-1}.[46] From this discussion, it can be concluded that the carbosilane groups present in our samples have $n = 1$.

5. Si−H. Si−H stretching bands were observed for all samples. Extensive investigations on this mode in Si-based materials have been carried out by Lucovsky and co-workers.[53,55] The HAr sample exhibited a single Si−H stretching band at 2125 cm^{-1}, while sample HO20 exhibited two well-distinguished bands at 2220 and at 2285 cm^{-1}.

6. N−H. The presence of N−H bonds within the networks investigated is inferred from both the N−H deformation and stretching bands. Sample HAr exhibited a small band at 1182 cm^{-1}, which is very close to the N−H deformation band observed for the HMDSN molecule.[41] As the oxygen flow rate increases, the intensity of this band decreases and, for sample HO20, it is only observed as a high-frequency tail of the strong AS1 band. Observing Figure 3, it is possible to notice a small band around 3370 cm^{-1}, which is attributed to the N−H stretching vibration.[52] With the increase in the oxygen flow rate, however, this band is distorted by the superimposition of the O−H stretching band.

7. C═O. The formation of C═O bonds is observed for samples HO10 and HO20 through the C═O stretching band at around 1710 cm^{-1}.[52] However, judging from the well-known strong infrared activity of this mode and the low intensity of this band for our films, it seems that the amount of this group is only marginal.

III.C. Oxygen Incorporation: Si−H Stretching Frequencies. The oxygen incorporation was interestingly investigated by means of the analysis of the Si−H stretching mode. Such a mode has proved to be sensitive both to the local environment and to remote effects, i.e., to the electronegativity of the atoms bonded to the same Si atom as the Si−H bond and to the overall "electronegativity" of the film. Extensive investigations on this matter have been carried out by Lucovsky and co-workers.[53,55]

In our films, Si−H moieties appeared as marginal components of all samples (see Figure 6). For sample HAr, it appears as a single band with a maximum at 2125 cm^{-1}. Such a value is compatible with a silicon polymer without oxygen bridges such as polymethylsilane (PMS).[54] The Si−H stretchings are more complex when we turn our attention to the other samples. The band splits into at least two bands with maxima at around 2220 and 2285 cm^{-1}. Sample HO2.5 even has a low-frequency shoulder at around 2150 cm^{-1}.

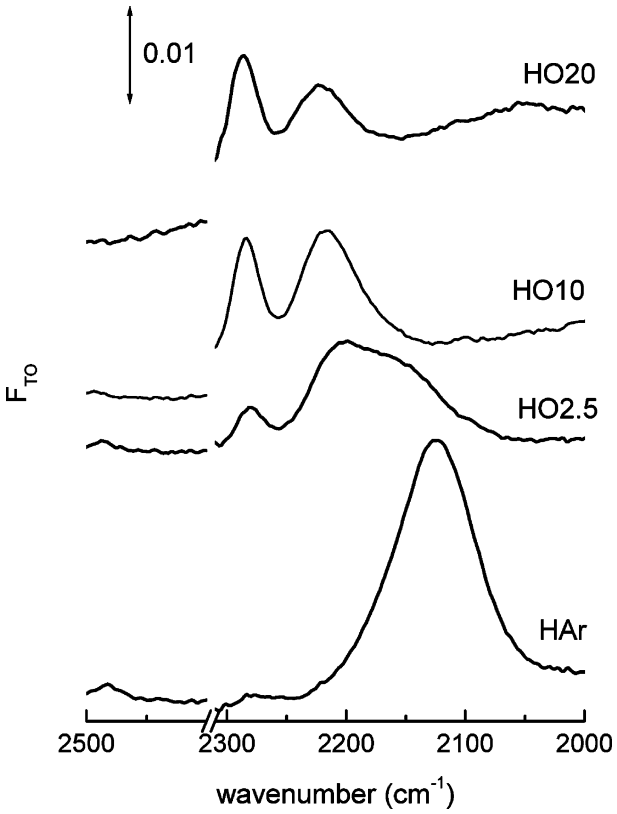

Figure 6. Magnification of the TO functions for all samples in the region of Si−H stretching.

The Si−H stretching bands positioned at lower wavenumbers are indicative of a silicon polymer with a low number of oxygen bridges whereas those positioned at higher wavenumbers are indicative of a highly oxidized silicon polymer.[53,55] These splittings are indicative of nonhomogeneity in the oxygen distribution throughout the network. This observation differs from what is amply indicated in the literature about the high structural homogeneity provided by plasma syntheses. It seems that the network is formed by very oxygen-bridge-rich domains and oxygen-bridge-poor domains. It is important to stress that, as far as a literature search revealed, this is the first time that Si−H stretching band splittings are observed for plasma polymers.

III.D. LO-TO Splittings. LO-TO splittings are sensitive both to the density of the corresponding oscillator and to its strength, the second factor being a *sine qua non* condition for its observation.[26] Therefore, LO-TO splitting is a very important phenomenon for strongly IR-active modes, such as the asymmetrical stretchings of metal−oxygen bonds, such as Ti−O,[34−37] Si−O,[13,14,27−33] and W−O.[38] C−H stretchings, for instance, which are not very strong modes, do not present an important LO-TO splitting.

Taking LO-TO splittings into account is very important when using infrared reflection−absorption spectroscopy using off-normal incidence angles.[13] That is because it is a very good condition for observing LO modes, a phenomenon known among spectroscopists as the Berreman effect,[19,23] and conventional IR band assignments are made through normal-incidence transmittance experiments.

Table 4 summarizes the observed LO-TO splittings (Δ_{LO-TO}) for our films. There was almost invariably splitting

(55) Lucovsky, G. *J. Non-Cryst. Solids* **1998**, *227*, 1.
(56) Ono, H.; Ikarashi, T.; Miura, Y.; Hasegawa, E.; Ando, K.; Kitano, T. *Appl. Phys. Lett.* **1999**, *74*, 203.

Table 4. LO-TO Splittings Observed for Some Modes

band	LO-TO splitt ing (cm^{-1})			
	HAr	HO2.5	HO10	HO20
ρ_{Me},ν_{SiC} in Si−Me_2	10	10	10	9
ρ_{Me},ν_{SiC} in Si−Me_3	11	9	10	8
$\nu_{AS,SiN}$ in Si−NH−Si	20	22	11	3
$\nu_{AS,SiO}$ in Si−O−Si		20	48	73
$\delta_{S,Me}$ in Si−Me_x	5	6	5	6

for the Si−C stretching modes for both $SiMe_2$ and $SiMe_3$ at around 10 cm^{-1}. Such splitting may have been observed due to Si^+-C^- polarity. A small Δ_{LO-TO} was also observed for the symmetrical deformation of Me in $SiMe_x$ groups.

The Δ_{LO-TO} for the Si−O asymmetrical stretching increased from 0 (samples HAr) to 73 cm^{-1}, while for the Si−N asymmetrical stretching it decreased from 20 (sample HAr) to 3 cm^{-1} (sample HO20). These observations signal an increase in the Si−O−Si network and a decrease in the Si−NH−Si network as the oxygen flow increased.

The TO spectra are practically insensitive to oxygen inclusion, as far as the AS1 band position is concerned. With an increase in the oxygen flow rate and consequent increase in the oxygen incorporation into the film, an increase in the AS1 band intensities and a decrease in the $SiMe_x$ bands are noticed. However, the LO spectra exhibit considerable band shifts when the Si−O−Si asymmetrical stretching is analyzed. The Δ_{LO-TO} is very sensitive to the oxygen incorporation, increasing with the O_2 flow rate increase. This is due to an increase in the Si−O−Si groups "concentration", allowing long-range interactions among these oscillators, as we have previously demonstrated.[13,14] However, differently from our previous studies,[13,14] it is noticeable how the LO-AS1 bands are more symmetrical in relation to their maxima, although they have high width at half-height ($\sim$120 cm^{-1}), i.e., of the same order of magnitude as that observed for highly oxidized films.[13,14] This behavior of the LO-AS1 bands can be associated with film heterogeneity, as was revealed by analysis of the Si−H stretching mode frequencies. It can be rationalized that, in the films studied here, there are domains that are enriched in Si−O−Si groups and domains that have lower Si−O−Si group densities. In the former, the Δ_{LO-TO} would be higher whereas in the latter, it would be lower, resulting in a broad LO band. This broadening is different from that which is observed for the AS1 band in vitreous silica, whose asymmetry is attributed to dangling bonds, Si−OH terminations, etc.

For the asymmetrical stretchings of Si−N−Si groups in the TO spectra, both their intensity and position are affected by oxygen incorporation, as discussed before. Their positions are a reflection of the different configurations of the silicon atoms bonded to the imide groups, as can be deduced from Table 3.

III.E. Film Structure. From the band assignments made above, we infer that our films are constituted of networks of interconnected silicon-centered distorted tetrahedra with three different bridging units: (i) imide groups, (ii) methylene groups, and (iii) oxygen atoms. As for network-terminating groups, we have basically methyl groups and hydrogen atoms, though the amount of the latter is very small. Even so, considering that the same silicon atom can be bonded to one or more of these bridging units, the structure of the tetrahedra present in our samples can be very diversified. In general, the physical properties of all samples show evidence of intense cross-linking since they are coherent, hard, and insoluble to common solvents such as propanol and acetone.

$$Si(CH_3)_xBU_{(2-0.5x)}$$

with $0 \le x \le 3$

BUs	Sample
CH_2, NH	HAr
CH_2, NH, O	HO2.5 and HO10
NH, O	HO20

Figure 7. Silicon-centered distorted tetrahedra present in the investigated films. BU stands for bridging unit.

Figure 7 summarizes the tetrahedra forming the films according to the conclusions drawn from the infrared analysis. We have observed a depletion in the incorporation of CH_2 bridges as a result of O_2 dilution of the plasma. Such a depletion has already been observed in our previous work on films deposited from plasmas of mixtures of HMDSO and O_2.[14] O_2 dilution also causes the incorporation of NH bridges to be diminished. From the infrared analysis, it is possible to affirm that the bridges present in film HAr are CH_2 and NH. For samples HO2.5 and HO10, all three possible bridges seem to occur, while for sample HO20, only NH and O bridges are incorporated. Therefore, this type of synthesis can be used to obtain materials with controllable amounts of these bridges.

IV. Conclusions

The present work describes the effects of diluting hexamethyldisilazane (HMDSN) vapor either in pure argon or in oxygen−argon mixtures on the solid film deposited from the resulting plasma. Such a dilution provides a manner of incorporating controllable amounts of Si−O groups into the solid film as shown by the RBS elemental analysis. The characterization of the films investigated here was made by longitudinal and transverse optical (LO and TO, respectively) functions in the mid-infrared calculated through the Kramers-Krönig analysis of transmittance spectra. The infrared analysis showed that the films were formed by silicon-centered distorted tetrahedra of the following type: $Si(CH_3)_xBU_{(2-0.5x)}$, where $0 \le x \le 3$ and BU stands for "bridging unit". For the sample deposited in the absence of O_2 in the discharge, BU = CH_2 and NH; for the samples deposited with an O_2 flow rate (f_{O2}) of 2.5 and 10 sccm, BU = CH_2, NH, and O; and for the sample deposited with f_{O2} of 20 sccm, BU = NH and O. The Δ_{LO-TO} for the Si−O asymmetrical stretching increased from 0 (f_{O2} = 0 sccm) to 73 cm^{-1} (f_{O2} = 20 sccm), while for the Si−N asymmetrical stretching it decreased from 20 (f_{O2} = 0 sccm) to 3 cm^{-1} (f_{O2} = 20 sccm). These observations signal an increase in the Si−O−Si network and a decrease in the Si−NH−Si network as the oxygen flow increased. An interesting

conclusion drawn from our analysis of the Si−H stretching mode position and Δ_{LO-TO} for the AS1 band is that the films deposited in the presence of O_2 are not structurally homogeneous, but have domains with different proportions of O bridges.

Acknowledgment. The Fundação de Amparo à Pesquisa do Estado de São Paulo − FAPESP (Grants # 98/11743-2, # 98/10979-2, and # 02/07482-6), the Conselho Nacional de Desenvolvimento Científico e Tecnológico − CNPq, and the Comissão de Aperfeiçoamento de Pessoal de Nível Superior − CAPES, are gratefully acknowledged for financial support. We are also indebted to Dr. Donald C. McKean for enlightening discussions about band assignments, to Dr. M. Isabel Felisberti for clarifying discussions regarding polymer terminology, to the Centro de Componentes Semicondutores (CCS) /Unicamp for allowing the use of the ellipsometer, and to Dr. Carol H. Collins for revising this manuscript.

Note Added after ASAP Publication. The caption to Figure 3 and the Table 3 title were incorrect in the version published ASAP August 2, 2005; the corrected version was published August 9, 2005.

CM050319O